J Vis (2010) 13:61–68
DOI 10.1007/s12650-009-0005-6

REGULAR PAPER

Y. Yamagishi · S. Kimura · Makoto Oki

Flow characteristics around a square cylinder with changing chamfer dimensions

Received: 3 April 2009 / Revised: 19 July 2009 / Accepted: 6 September 2009 / Published online: 8 January 2010

Abstract It is known that for a square cylinder subjected to uniform flow, the drag force changes with the angle of attack. To clarify the flow characteristics around a square cylinder with corner cutoffs, we measured the drag coefficient and the Strouhal number for changing chamfer dimensions. We analyzed the flow around a square cylinder with corner cutoffs by applying the RNG k–ε turbulent model, and investigated the surface flow pattern using visualization by means of the oil film and mist flow method. From these results, we obtained the surface flow patterns by the oil film method and numerical analysis. The numerical results agreed well with the experimental values. The drag coefficient of the square cylinder with corner cutoffs decreased suddenly at an angle of attack of about $\alpha = 0°$– $10°$ when compared with the drag coefficient for a square cylinder. The minimum value of the drag coefficient for the square cylinder with corner cutoffs decreased by about 30% compared with that for the square cylinder. The drag coefficient of the square cylinder with 10% corner cutoffs was found to be smallest, since the wake area of this square cylinder was smaller compared with that of the other square cylinder.

Keywords Square cylinder with corner cutoffs · Drag · Oil film · Mist flow · Numerical analysis

1 Introduction

It is known that the maximum value of the drag coefficient of a square cylinder is about 2 at zero angle of attack, but that of a circular cylinder is about 1.2, and the drag coefficient of a square cylinder increases by about 60% compared with that of a circular cylinder. There are many structures with square cylinder shapes, such as high-rise buildings, to which we can apply the theoretical study of drag reduction of a square cylinder to reduce wake flow and wind load. A square cylinder was examined experimentally (Igarashi 1984; Shao et al. 2007). A square cylinder with grooves and tabs was examined (Koide et al. 2006; Layukallo and Nakamura 2003; Yamagishi et al. 2004). A square cylinder with rectangular cutouts at its edges was examined experimentally (Kurata and Morishita 1998). However, there has been no complete investigation into the effect of corner cutoffs on the flow characteristics around a square cylinder.

In this study, we examined the flow characteristics around a square cylinder with corner cutoffs for changing chamfer dimensions and angles of attack using experiments, numerical analysis, and visualization.

Y. Yamagishi (✉) · S. Kimura
Department of Mechanical Engineering, Kanagawa Institute of Technology,
1030 Shimoogino, Atugi, Kanagawa 243-0292, Japan
E-mail: yamagisi@me.kanagawa-it.ac.jp

M. Oki
School of High-Technology for Human Welfare, Tokai University, 317 Nishino, Numazu,
Shizuoka 410-0395, Japan

2 Experimental method and numerical analysis

2.1 Experimental apparatus

Figure 1 shows the square cylinder with corner cutoffs used for this experiment. The cylinder was made of aluminum and was 420 mm in length with 30 × 30 mm cross-sectional dimensions d. C1, C3, and C5 designate cylinders that have chamfers with lateral dimensions of 1, 3, and 5 mm cut along the corners of each square cylinder, as shown in Fig. 1.

Figure 2 shows the schematic diagram of the experimental apparatus. We conducted the experiments in a 400 mm × 400 mm circulating wind tunnel with a turbulence intensity of about 0.65% and a maximum speed of around 35 m/s. We placed the cylinder vertically in the measuring section of the wind tunnel. The flow around the cylinder was examined for Reynolds numbers $Re = Ud/v$ (d is the side length of the cross section of the cylinder, U the uniform flow velocity, and v is the kinematic viscosity) ranging from 1×10^3 to 6×10^4.

2.2 Measurement and visualization

We obtained the drag from the change in momentum in front of and behind the cylinder. Measurements of the mean velocity were made using an IHW hot-wire anemometer (sampling time 1 ms, number of data 1,024) by moving the hot-wire probe at intervals of 10 mm in the y-axis direction. We digitized the output signals on a personal computer. Initially we obtained the drag coefficients $C_D = D/(d\rho U^2/2)$ (D is the drag per unit d, ρ is density of air) of the square cylinder using this drag measurement method. We confirmed that these drag coefficients C_D equaled the drag coefficients of a square cylinder (Lee 1975; Ohtsuki et al. 1978), and then proceeded to obtain the drag coefficients C_D of the square cylinder with corner cutoffs. We used the IHW to measure the frequency of the generating vortex f. We observed the flow around the cylinder made visible by means of a propylene glycol mixture mist as a tracer. We painted the surface of the cylinder black and covered it with a white oil film dissolved in a solution of titanium oxide composed of liquid paraffin and oleic acid. We took photographs of the cylinder surface and around the cylinder using a digital camera and a video camera.

2.3 Numerical analysis

We performed numerical analysis with the versatile fluid analysis software package, Fluent 6.3, using the finite volume method. The analysis was made in unsteady two-dimensional turbulent flow. The RNG k–ε model was used as a turbulent model. Figure 3 shows a complete view of the mesh and boundary conditions.

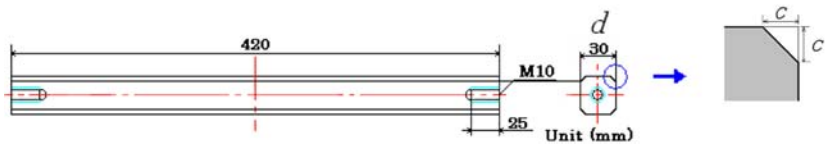

Type	Cutoff length C(mm)	C/d
Square cylinder	0	0
C1	1	0.033
C3	3	0.1
C5	5	0.167

Fig. 1 Test cylinders

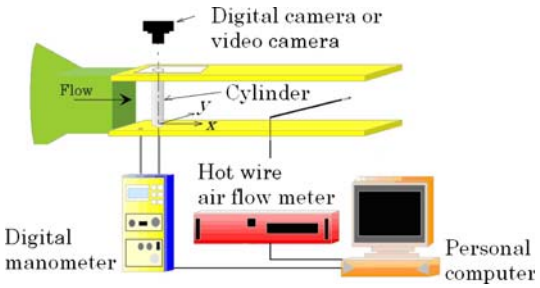

Fig. 2 Experimental apparatus and instruments

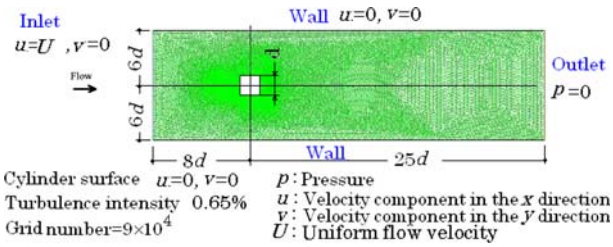

Fig. 3 Whole meshes and boundary conditions

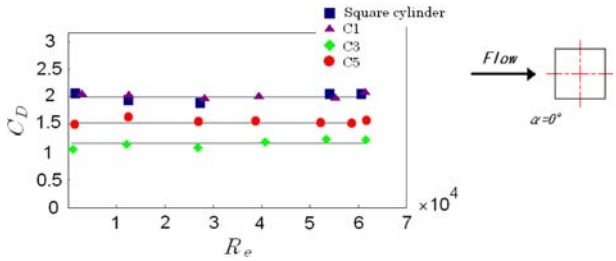

Fig. 4 Drag coefficient of square cylinders with corner cutoffs and square cylinder versus Reynolds number

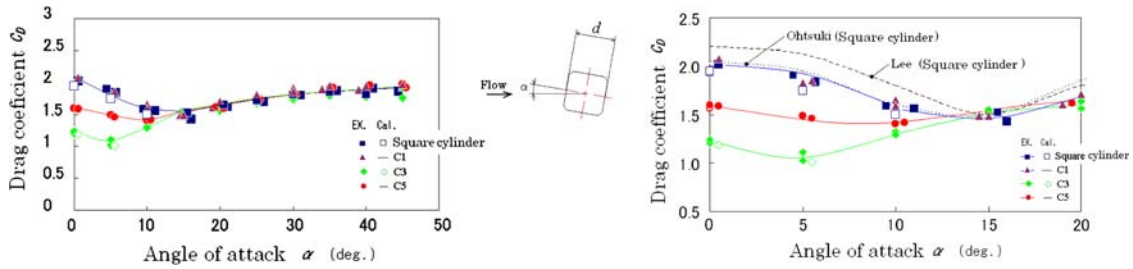

Fig. 5 Drag coefficient of square cylinders with corner cutoffs and square cylinder

3 Results and discussion

The variations in the mean drag coefficient C_D (angle of attack $\alpha = 0°$) by the experiment with Reynolds number for square cylinder, C1, C3 and C5 in the range of $Re = 1 \times 10^3$–6×10^4 are shown in Fig. 4. It turns out that a drag coefficient is a constant value in the range of $Re = 1 \times 10^3$–6×10^4.

Figure 5 shows the variations in the mean drag coefficients C_D with the angle of attack α for cylinders at a Reynolds number $Re = 6 \times 10^4$. The figure on the right-hand side is an enlarged figure. The mean drag coefficient of the numerical analysis performed the time average by the cycle of the fluctuating lift. The measurement on a square cylinder (Lee 1975; Ohtsuki et al. 1978) is also included for comparison. The drag coefficient of C1 is almost the same value as the square cylinder. The sudden decrease of C_D occurs at about $\alpha = 0°$–$10°$ in the case of the C3 and C5 cylinders compared with the square cylinder. Further, the drag of C3 is less than that of C5. The minimum value of the drag coefficient C_D for the C3 cylinder decreases by about 30% compared with that for the square cylinder. The results of the numerical analysis show a tendency to agree well with the experimental values.

Figure 6 shows the variations of C_D with the chamfer dimension C for four kinds of cylinders at $\alpha = 0°$ for $Re = 6 \times 10^4$. The value of C_D of each cylinder is a constant value of about 2 in the range of $C/d = 0$ (square cylinder) $\sim$0.033 (C1 cylinder), then falls abruptly to a minimum value of about 1.2 at $C/d = 0.1$ (C3 cylinder), and then increases slightly.

Figure 7 shows the flow patterns around the square, C3 and C5 cylinders, which were made visible using the propylene glycol mixture mist flow at $\alpha = 0°$ for $Re = 1 \times 10^3$. The picture is an instantaneous photograph of unsteady flow.

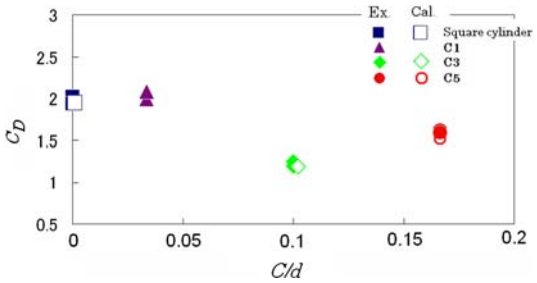

Fig. 6 Drag coefficient of cylinders at $\alpha = 0°$

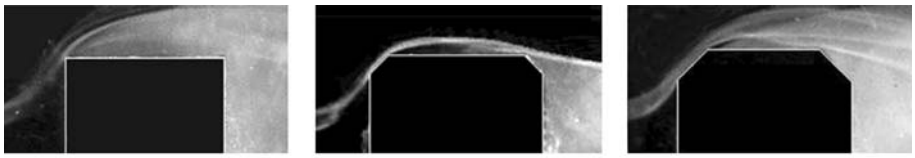

Fig. 7 The flow patterns around the cylinder using the propylene glycol mixture mist flow. **a** Square cylinder, **b** C3 cylinder, **c** C5 cylinder

Figure 8 shows the computational results of the streamlines around the square cylinder for the C3 and C5 cylinders for $Re = 6 \times 10^4$. The figure is an instantaneous streamlines of unsteady flow. The flow patterns obtained using the mist flow and numerical analysis methods agree well.

In the separation areas of the side face of a square cylinder and square cylinder with cutoffs, the area of C3 is small compared with the square and C5 cylinders.

Figure 9 shows the flow patterns along the square, C3 and C5 cylinder surfaces that were made visible using the white oil film method at $\alpha = 0°$ for $Re = 6 \times 10^4$.

In addition, Fig. 10 shows the shear stress by numerical analysis at the D corner for $Re = 6 \times 10^4$. Both the A and D corners of the square cylinders with corner cutoffs show peeling of the white oil film by forward flow. Peeling of a white oil film is the black portion shown by the red arrows. The peeling area of the white oil film of C5 is large compared with that of C3, and the shear stress is large. We checked the shear stress by numerical analysis. Large value of the shear stress of C5 is red. We also noted that the tangential velocity of the corner end side of C5 becomes large compared with C3, and enlarges the separation area of the cylinder side face.

The computational results of the time mean values of velocity distributions at the front face of the cylinder to the $0.3d$ position on the cylinder side surface at $Re = 6 \times 10^4$ are shown in Fig. 11. The ordinate shows y/d (y is the distance from the center of the cylinder to the measurement position and d the width of the cylinder) and the abscissa shows u/U (u is the velocity component in the x direction and U the uniform velocity). The velocity distribution on the cylinder surface for the C3 cylinder becomes larger compared with the square cylinder and the C5 cylinder.

The experimental results of the velocity distributions u/U (u is velocity component in the x direction) at $x/d = 16$ behind the cylinders at $\alpha = 0°$ for $Re = 6 \times 10^4$ are shown in Fig. 12. The velocity of C1 is almost the same value as the square cylinder. The value of the velocity behind the C3 cylinder at $\alpha = 0°$ becomes large. The large velocity behind the cylinder decreases the drag coefficient.

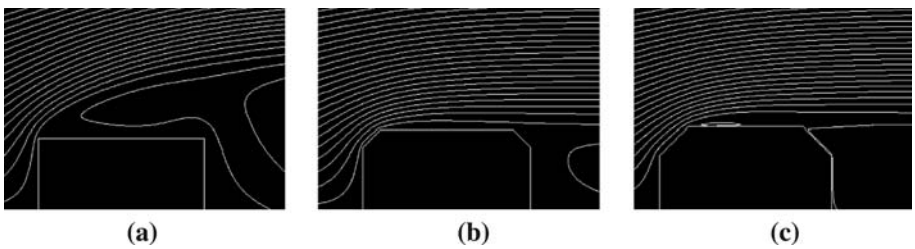

Fig. 8 The computational results of the streamlines around the cylinder. **a** Square cylinder, **b** C3 cylinder, **c** C5 cylinder

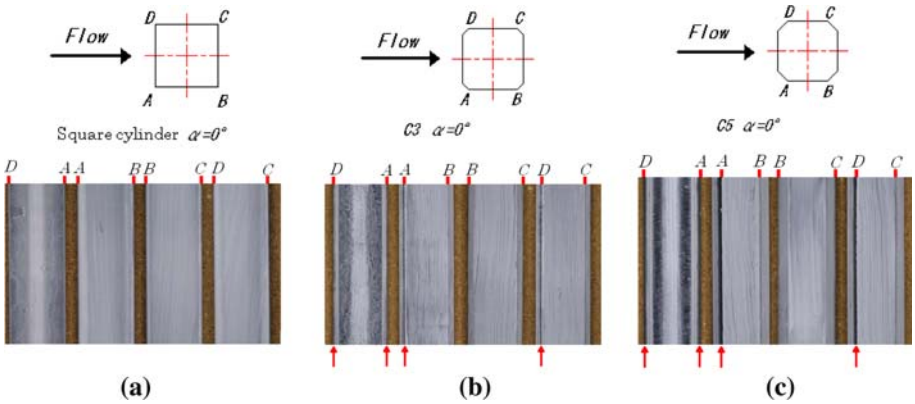

Fig. 9 Oil-pattern along the cylinders. **a** Square cylinder, **b** C3 cylinder, **c** C5 cylinder

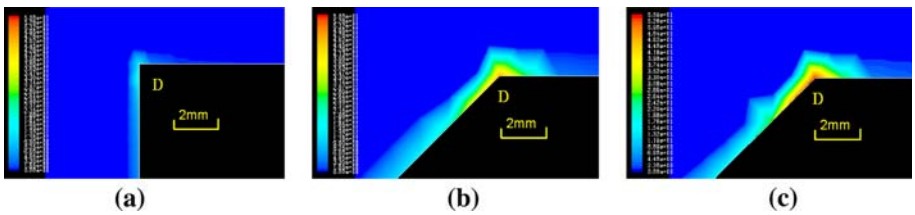

Fig. 10 The computational results of the shear stress around the cylinder. **a** Square cylinder, **b** C3 cylinder, **c** C5 cylinder

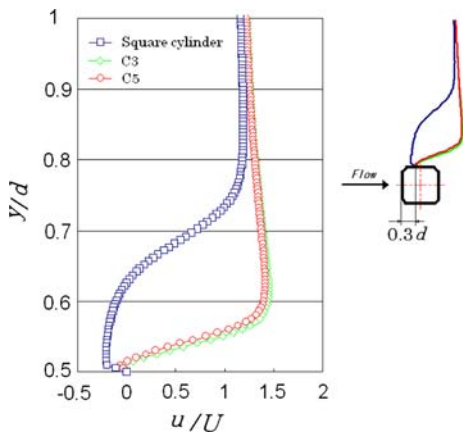

Fig. 11 The computational results of the velocity distribution on the cylinder surface

The time mean values of turbulent kinetic energy k distributions around the square, C3 and C5 cylinders at $\alpha = 0°$ and for $Re = 6 \times 10^4$ are shown in Fig. 13. The maximum value of the turbulent kinetic energy around the square cylinder becomes large compared with that for the C3 and C5 cylinders.

The computational results of the time mean values of pressure distributions around the square, C3 and C5 cylinders at $\alpha = 0°$ for $Re = 6 \times 10^4$ are shown in Fig. 14. The pressure on the downstream side of the square cylinder becomes smaller than on the downstream side of C3 and C5 cylinders.

Figure 15 shows the experimental and computational results of the mean pressure distributions along the square, C3 and C5 cylinders at $\alpha = 0°$ for $Re = 6 \times 10^4$. The figure on the right-hand side is an enlarged figure. The ordinate shows the pressure coefficient, and the abscissa shows the angle from the stagnation point θ.

The results of the numerical analysis agree well with the experimental values. The pressure coefficient of the square cylinder is a large value, while that of the C3 is a small value on the part of the front face at about $\theta = -45°$ to $+ 45°$. The pressure coefficient of the square cylinder is a small value, while that of the C3 and

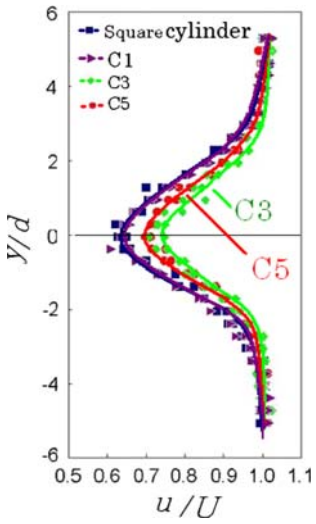

Fig. 12 The experimental results of the velocity distribution behind the cylinder

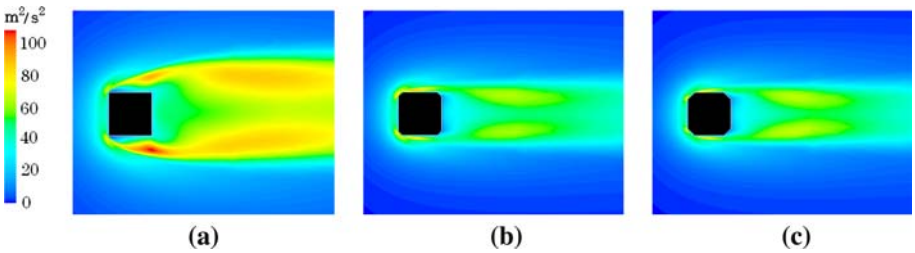

Fig. 13 The time mean values of the turbulent kinetic energy distributions around the cylinder. **a** Square cylinder, **b** C3 cylinder, **c** C5 cylinder

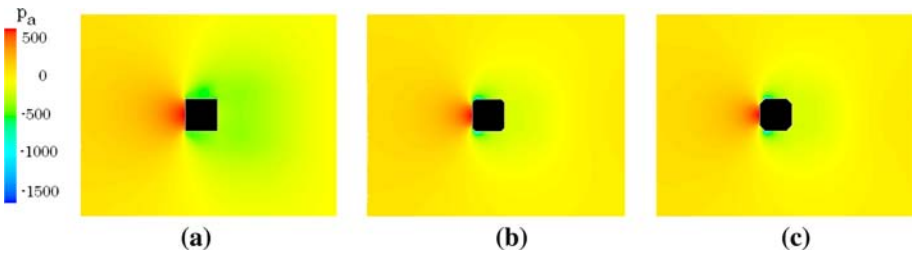

Fig. 14 The time mean values of the pressure distributions around the cylinder. **a** Square cylinder, **b** C3 cylinder, **c** C5 cylinder

C5 are large values on the part of the side and back face at about $\theta = 90°$–$270°$, hence the drag coefficient of C3 becomes small.

Figure 16 shows the variations of C_D with the width of the wake for the three kinds of cylinders at $\alpha = 0°$ for $Re = 1 \times 10^3$. The ordinate shows the drag coefficient C_D. The abscissa shows the visualization results of the width of the wake b/d (b is the width of wake and d is the side of the cross section of the cylinder) at $l/d = 1.5$ behind the cylinders (l is the distance of the central axis of the cylinder to b). It is clear that the drag coefficient becomes large as the width of the wake becomes large at $\alpha = 0°$.

Figure 17 shows the variations in the Strouhal number St ($St = fd/U$, f is the frequency of generating vortex which was counted from the excellence frequency of the power spectrum using the hot-wire anemometer, d the side length of the cross section of the cylinder, and U is the uniform velocity) with an angle of attack α for the cylinders at a Reynolds number $Re = 6 \times 10^4$. We found that the Strouhal numbers of C3 and C5 become large compared with that of the square cylinder in the range of $\alpha = 0°$–$15°$. The Strouhal number of C3 is the almost same value as C5.

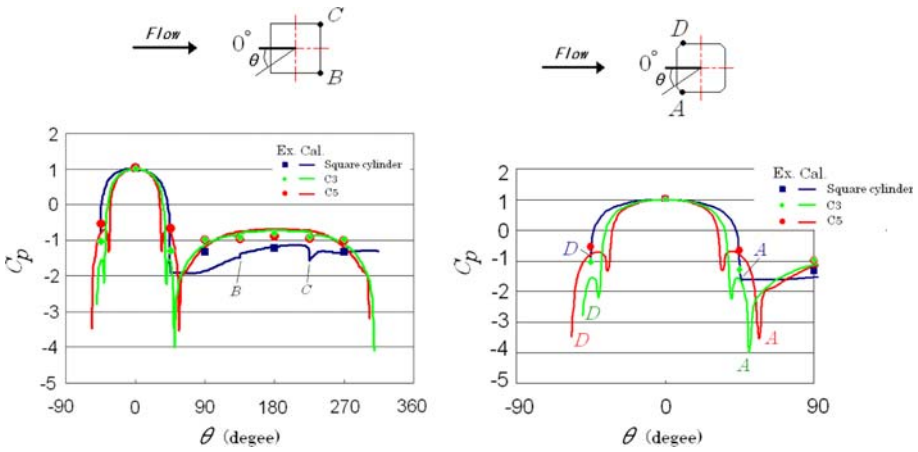

Fig. 15 The pressure distributions along the cylinder

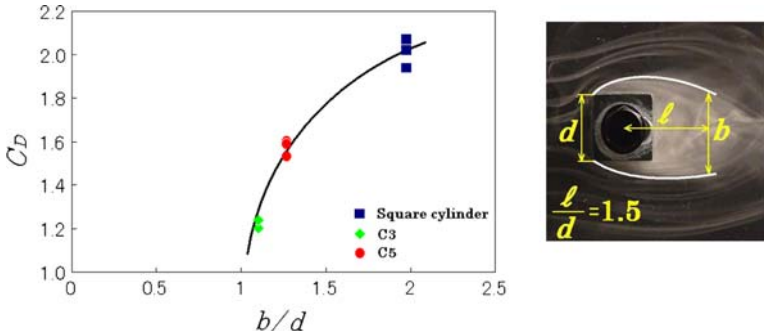

Fig. 16 Drag coefficient with the non-dimensional width of wake for cylinders

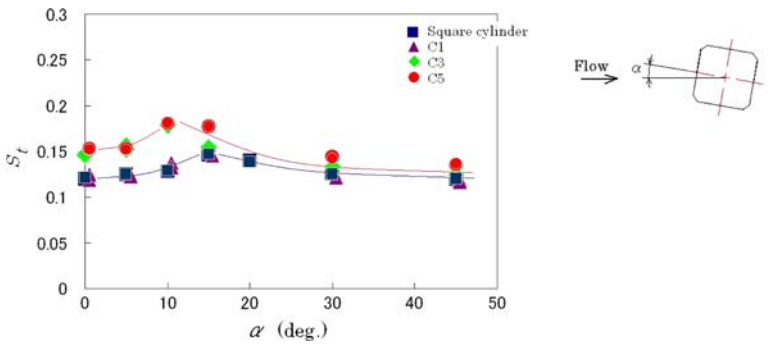

Fig. 17 Relationship between Strouhal number and angle of attack

4 Conclusions

The results of the experiments and the numerical analysis around square cylinders with corner cutoffs in the range of $Re = 1 \times 10^3$–6×10^4 lead to the following conclusions:

1. The sudden decrease of C_D occurs at about an angle of attack $\alpha = 0°$–$10°$ in the case of the C3 and C5 cylinders compared with that of the square cylinder. The minimum value of the drag coefficient C_D for the C3 cylinder decreases by about 30% compared with that of the square cylinder.
2. The value of C_D of each cylinder for an angle of attack 0° is a constant value of about 2 in the range of $C/d = 0$ (Square cylinder) ~ 0.033 (C1 cylinder), (C is the chamfer dimension), falls abruptly to a minimum value of about 1.2 at $C/d = 0.1$ (C3 cylinder), and then increases slightly.

3. It is clear that the tangential velocity of the corner end side of C5 becomes large compared with C3, and enlarges the separation area of square cylinder side face.

References

Igarashi T (1984) Characteristics of the flow around square prisms. Trans Jpn Soc Mech Eng 50(449):210–218
Koide M, Okanaga H, Aoki K (2006) Drag reduction effect of square cylinders by grooves and corner-cuttings. J Visualization Soc Jpn 26(1):69–72
Kurata M, Morishita T (1998) Drag reduction of a bluff body with small cutout at its edges. Trans Jpn Soc Mech Eng 64(618):397–404
Layukallo T, Nakamura Y (2003) Passive separation control on a square cylinder at transonic speed. Trans Jpn Soc Aeronaut Space Sci 45(150):236–242
Lee BE (1975) The effect of turbulence on the surface pressure field of a square prism. J Fluid Mech 69(2):263–282
Ohtsuki S, Fujii K, Washizu K, Ohya T (1978) Wind tunnel experiments on aerodynamic forces and pressure distributions of rectangular cylinders in a uniform flow. Symp Jpn Assoc Wind Eng 5:169–176
Shao CP, Wang JM, Wei QD (2007) Visualization study on suppression of vortex shedding from a cylinder. J Visualization 10(1):57–64
Yamagishi Y, Akaike S, Nemoto M (2004) Effect of the grooves on flow characteristics around a square prism. 52th Symposium of turbomachinery Society of Japan, Niigata, pp 118–123